IOPscience iopscience.iop.org

Home Search Collections Journals About Contact us My IOPscience

An extremely efficient and rapid algorithm for numerical evaluation of three-centre nuclear attraction integrals over Slater-type functions

This article has been downloaded from IOPscience. Please scroll down to see the full text article.

2003 J. Phys. A: Math. Gen. 36 11791

(http://iopscience.iop.org/0305-4470/36/47/007)

View the table of contents for this issue, or go to the journal homepage for more

Download details:
IP Address: 171.66.16.89
The article was downloaded on 02/06/2010 at 17:16

Please note that terms and conditions apply.

INSTITUTE OF PHYSICS PUBLISHING JOURNAL OF PHYSICS A: MATHEMATICAL AND GENERAL

J. Phys. A: Math. Gen. **36** (2003) 11791–11805 PII: S0305-4470(03)63584-5

An extremely efficient and rapid algorithm for numerical evaluation of three-centre nuclear attraction integrals over Slater-type functions

Lilian Berlu and Hassan Safouhi

Faculté Saint-Jean/University of Alberta, 8406, 91 Street, Edmonton, Alberta T6C 4G9, Canada

E-mail: hassan.safouhi@ualberta.ca and lilian.berlu@chimsrv1.univ-bpclermont.fr

Received 16 May 2003, in final form 10 September 2003
Published 12 November 2003
Online at stacks.iop.org/JPhysA/36/11791

Abstract

The present work concerns the development of an extremely accurate and rapid algorithm for the numerical evaluation of the three-centre nuclear attraction integrals over Slater-type functions. These integrals are numerous, they occur in many millions of terms, even for small molecules and they require rapid and accurate evaluation. The new algorithm is based on nonlinear transformation methods, on numerical quadrature and on properties of the sine and Bessel functions. The section with numerical results shows the high accuracy and the substantial gain in calculation time realized using the new algorithm. The complete expressions of the three-centre nuclear attraction integrals over B functions and over Slater-type functions are evaluated for different values of the quantum numbers to show the efficiency of the new approach. Numerical results obtained with linear and nonlinear systems and comparisons with numerical results from the literature are listed.

PACS numbers: 02.30.Gp, 02.60.Gf, 02.60.Jh, 31.15.Ar, 31.15.Qg

1. Introduction

It is well known that in any *ab initio* molecular orbital (MO) calculation [1], the major task involves the computation of molecular integrals, among which the computation of three-centre nuclear attraction integrals is most frequently encountered. As the molecular system gets larger, computation of these integrals becomes one of the most laborious and time-consuming steps in molecular system calculation. Improvement of the computational methods of molecular integrals would be indispensable to further development in computational studies of large molecular systems.

 © 2003 IOP Publishing Ltd Printed in the UK

In *ab initio* calculations using the LCAO-MO approximation [2], MOs are built from a linear combination of atomic orbitals. Thus, the choice of a reliable basis functions is of prime importance in accurate molecular integral calculations. A good atomic orbital basis should decay exponentially for large distances [3] and should also satisfy Kato's conditions for analytical solutions of the appropriate Schrödinger equation [4].

The most popular functions used in *ab initio* calculations are the so-called Gaussian-type functions (GTFs) [5]. With GTFs, the numerous molecular integrals can be evaluated rather easily. Unfortunately, these GTF basis functions fail to satisfy the above mathematical conditions for atomic electronic distributions.

Slater-type functions (STFs) [6, 7] satisfy the aforementioned mathematical requirements, but their use as a basis set of atomic orbitals has been prevented by the fact that their multicentre integrals turned out to be extremely difficult to evaluate for polyatomic molecules. We note that many researchers hope that the next generation of *ab initio* programmes will be based on the usage of STFs [8, 9], therefore it does not seem impossible to envisage that STFs may compete with GTFs [5] in accurate and rapid molecular calculations in the near future. Indeed, much effort is being made to develop efficient molecular algorithms for integrals over conventional STFs or other related basis functions (see [10–13] and references therein).

The B functions [14–16] have some remarkable mathematical properties applicable to multicentre integral problems. They possess a relatively simple addition theorem [16, 17] and their Fourier transform is of exceptional simplicity [18]. The B functions are well adapted to the Fourier transformation method [19, 20]. Note that STFs can be expressed as linear combinations of these functions [15].

All these properties led to a considerable amount of research on B functions and their molecular multicentre integrals [21–31].

The Fourier transformation method, which is one of the most successful approaches applied to multicentre integrals over B functions, allowed analytical expressions for the three-centre nuclear attraction integrals to be developed. These analytic expressions involve two-dimensional integral representations. The inner semi-infinite integrals are highly oscillatory, due to the presence of the spherical Bessel function $j_\lambda(vx)$ in the integrands. These semi-infinite integrals are to be evaluated via a numerical quadrature of integral representations in terms of *nonphysical* integration variables.

In previous work [23–25], we have demonstrated the efficiency of the nonlinear $\bar{D}$ transformation of Sidi [32, 33], compared with the epsilon algorithm of Wynn and Levin's u transform, in evaluating this kind of semi-infinite integrals. Unfortunately, the calculation of the approximation $\bar{D}_n^{(4)}$ presents severe numerical and computation difficulties when dealing with molecular multicentre integrals especially when the values of the quantum numbers are large. In [26–28], we used a second-order linear differential equation satisfied by the integrand and which was obtained by Sidi [32, 37]. This led to the approximation $\bar{D}_n^{(2)}$ for the semi-infinite integrals under consideration. This led to a substantial gain in the calculation times, but it is still necessary for the calculations to compute the $(n + 1)$ successive zeros of the spherical Bessel function and a method to solve a set of linear equations.

In the present work, we used the $S\bar{D}$ approach [29] for the numerical evaluation of the semi-infinite highly oscillatory integrals involving spherical Bessel functions. The main idea of this approach consists in replacing the spherical Bessel function by the simple sine function, using a property that relates these two functions and in applying the $\bar{D}$ transformation [32, 33]. It is known that numerical integration of oscillatory integrands is difficult, but with the help of the nonlinear $\bar{D}$ transformation one can compute this kind of integrals to a high accuracy. Note that different techniques based on nonlinear transformations for improving convergence

Table 1. Values with 15 correct decimals of $\tilde{\mathcal{I}}(s)$ (7) obtained using the infinite series with the sine function (11).

s	ν	n_γ	n_x	λ	R_1	v	nmax	$\tilde{\mathcal{I}}(s)^{\text{nmax}}$	Time
0.240(−2)	5/2	1	1	0	34	32.0048	3748	0.681 713 239 241 357(−3)	53.76
0.998(0)	5/2	1	1	0	34	33.9960	4361	0.151 864 762 852 243(−2)	62.57
0.998(0)	9/2	3	2	1	30	29.9960	4433	0.590 113 822 812 245(−2)	97.51
0.240(−2)	9/2	3	2	2	45	43.0048	5383	0.103 067 574 467 870(−2)	136.01
0.240(−2)	15/2	6	4	3	50	48.0048	8022	0.160 307 326 565 246(−2)	229.18
0.998(0)	15/2	6	4	3	50	49.9960	9152	0.177 013 372 443 209(−1)	261.87
0.240(−2)	17/2	9	5	4	55	53.0048	8515	0.685 144 224 550 293(−3)	277.81
0.998(0)	17/2	9	5	4	55	54.9960	9681	0.243 705 341 101 324(−1)	315.56

$R_2 = 2.0$, $\zeta_1 = 1.5$ and $\zeta_2 = 1.0$. Numbers in parentheses represent powers of 10.

Table 2. Evaluation of $\tilde{\mathcal{I}}(s)$ (7).

nmax	$\tilde{\mathcal{I}}(s)^a$	Error^a	Time	n	$\tilde{\mathcal{I}}(s)^b$	Error^b	Time
3376	0.681 713 2392(−3)	0.43(−15)	55.44	3	0.681 713 2392(−3)	0.48(−16)	0.04
3922	0.151 864 7628(−2)	0.77(−15)	64.45	3	0.151 864 7628(−2)	0.35(−16)	0.04
4330	0.590 113 8228(−2)	0.76(−13)	92.27	3	0.590 113 8228(−2)	0.37(−14)	0.07
5539	0.103 067 5744(−2)	0.45(−13)	141.97	6	0.103 067 5744(−2)	0.19(−13)	0.14
8599	0.160 307 8325(−2)	0.50(−08)	248.17	3	0.160 307 3265(−2)	0.11(−15)	0.09
9853	0.177 013 8281(−1)	0.45(−07)	283.86	3	0.177 013 3724(−1)	0.68(−14)	0.09
9555	0.685 331 7643(−3)	0.18(−06)	309.80	3	0.685 144 2245(−3)	0.26(−15)	0.09
10927	0.243 733 6995(−1)	0.28(−05)	354.25	3	0.243 705 3411(−1)	0.42(−13)	0.10

R_2, ζ_1, ζ_2, s, ν, n_γ, n_x, λ, R_1 and v are given in table 1. The values $\tilde{\mathcal{I}}(s)^a$ were obtained using the infinite series with spherical Bessel function (8). The values $\tilde{\mathcal{I}}(s)^b$ were obtained using $S\bar{D}_n^{(2,0)}$.

of highly oscillatory integrals including Bessel function integrals and algorithms for their efficient computation are presented in [34–39].

Using properties of the sine function, in particular the fact that its zeros are equidistant allowed the use of Cramer's rules as demonstrated by Sidi [32]. This result led to a development of a very simple and rapid algorithm for accurate numerical evaluation of the semi-infinite integrals of interest. Recurrence relations are developed for a better control of the degree of accuracy and to further reduce the calculation times. Numerical and computational studies are presented and discussed for a better stability of the algorithm. Practical formulae for the accurate numerical evaluation of the semi-infinite integrals under considerations are developed.

The symbol $S\bar{D}$ specifies that the semi-infinite integrals involving spherical Bessel functions are transformed into semi-infinite integrals involving the sine function and the nonlinear $\bar{D}$ transformation is applied with a second-order differential equation.

The complete expressions of the three-centre nuclear attraction integral over B functions and over STFs are evaluated for different values of the quantum numbers and with molecules NCCH and NCCCH. We compared the numerical results obtained using the new algorithm with those obtained by Grotendorst and Steinborn [20] (see table 11), by Bouferguene *et al* [11, 21, 12] (see tables 12–14). We also compared our numerical results with those obtained with the Alchemy package [40] (see tables 12 and 13).

The calculation times are listed (see tables 1–6) to show the rapidity and the efficiency of the new algorithm.

Table 3. Evaluation of $\tilde{\mathcal{I}}(s)$ (7).

n	$\tilde{\mathcal{I}}(s)^c$	Error ^{c}	Time	n	$\tilde{\mathcal{I}}(s)^d$	Error ^{d}	Time
10	0.681 713 2392(−3)	0.31(−15)	0.14	4	0.681 713 2392(−3)	0.41(−16)	1.00
10	0.151 864 7628(−2)	0.13(−14)	0.17	4	0.151 864 7628(−2)	0.20(−16)	1.10
10	0.590 113 8227(−2)	0.28(−12)	0.18	6	0.590 113 8228(−2)	0.94(−14)	2.64
10	0.103 067 5744(−2)	0.11(−14)	0.17	8	0.103 067 5744(−2)	0.15(−12)	4.14
10	0.160 307 3265(−2)	0.23(−12)	0.18	8	0.160 307 2959(−2)	0.30(−09)	4.90
10	0.177 013 3723(−1)	0.72(−11)	0.21	8	0.177 013 3766(−1)	0.41(−09)	5.32
10	0.685 144 2241(−3)	0.39(−12)	0.18	10	0.685 144 2194(−3)	0.50(−11)	7.14
10	0.243 705 3406(−1)	0.40(−10)	0.21	12	0.243 705 3409(−1)	0.10(−10)	7.75

$R_2, \zeta_1, \zeta_2, s, \nu, n_\gamma, n_x, \lambda, R_1$ and v are given in table 1. The values $\tilde{\mathcal{I}}(s)^c$ were obtained using $\bar{D}_n^{(2)}$. The values $\tilde{\mathcal{I}}(s)^d$ were obtained using $\bar{D}_n^{(4)}$.

Table 4. Values with 15 correct decimals of $\tilde{\mathcal{I}}(s)$ (7) obtained using the infinite series with the sine function (11).

s	ν	n_γ	n_x	λ	R_1	v	nmax	$\tilde{\mathcal{I}}(s)^{\text{nmax}}$	Time
0.240(−2)	5/2	5	1	0	3.5	0.4916	29	0.137 372 578 714 580(0)	1.42
0.998(0)	5/2	5	1	0	3.5	2.9930	179	0.233 410 511 641 676(−3)	2.70
0.240(−2)	7/2	3	1	0	4.5	1.4892	84	0.108 695 782 913 793(0)	1.20
0.998(0)	7/2	7	1	0	4.5	2.9910	141	0.148 098 914 431 698(−3)	2.25
0.998(0)	5/2	5	1	1	3.5	2.9930	169	0.366 428 166 959 532(−3)	3.62
0.240(−2)	7/2	5	3	2	5.5	2.4868	124	0.794 299 215 362 742(−2)	2.90
0.240(−2)	11/2	9	4	3	5.5	2.4868	133	0.697 423 068 145 726(0)	3.79

$R_2 = 3.0$, $\zeta_1 = 1.5$ and $\zeta_2 = 2.0$.

Table 5. Evaluation of $\tilde{\mathcal{I}}(s)$ (7).

nmax	$\tilde{\mathcal{I}}(s)^a$	Error ^{a}	Time	n	$\tilde{\mathcal{I}}(s)^b$	Error ^{b}	Time
29	0.137 372 5787(0)	0.555(−16)	1.48	9	0.137 372 5787(0)	0.846(−12)	0.21
173	0.233 410 5116(−3)	0.282(−15)	3.11	3	0.233 410 5165(−3)	0.488(−11)	0.04
83	0.108 695 7829(0)	0.444(−15)	1.46	11	0.108 695 7829(0)	0.138(−11)	0.14
136	0.148 098 9144(−3)	0.549(−15)	2.47	3	0.148 098 9195(−3)	0.516(−11)	0.04
173	0.366 428 1669(−3)	0.445(−15)	3.37	6	0.366 428 1791(−3)	0.122(−10)	0.12
128	0.794 299 2153(−2)	0.273(−14)	3.13	43	0.794 299 2182(−2)	0.287(−10)	0.79
141	0.697 423 0681(0)	0.247(−11)	3.91	53	0.697 423 0681(0)	0.105(−10)	1.10

$R_2, \zeta_1, \zeta_2, s, \nu, n_\gamma, n_x, \lambda, R_1$ and v are given in table 3. The values $\tilde{\mathcal{I}}(s)^a$ were obtained using the infinite series with spherical Bessel function (8). The values $\tilde{\mathcal{I}}(s)^b$ were obtained using $S\bar{D}_n^{(2,0)}$.

2. General definitions and properties

The STFs are defined in normalized form according to the following relationship [6, 7]:

$$\chi_{n,l}^m(\zeta, \vec{r}) = \sqrt{\frac{(2\zeta)^{2n+1}}{(2n)!}} r^{n-1} \, \mathrm{e}^{-\zeta r} Y_l^m(\theta_{\vec{r}}, \varphi_{\vec{r}}) \tag{1}$$

where n, l, m are the quantum numbers and where $Y_l^m(\theta, \varphi)$ stands for the surface spherical harmonic [41].

Table 6. Evaluation of $\tilde{\mathcal{I}}(s)$ (7).

n	$\tilde{\mathcal{I}}(s)^c$	Error ^{c}	Time	n	$\tilde{\mathcal{I}}(s)^d$	Error ^{d}	Time
10	0.137 372 5787(0)	0.15(−12)	0.25	3	0.137 372 5787(0)	0.15(−11)	0.75
10	0.233 410 5103(−3)	0.13(−11)	0.15	3	0.233 410 5116(−3)	0.14(−15)	0.65
12	0.108 695 7829(0)	0.53(−11)	0.21	3	0.108 695 7829(0)	0.23(−11)	0.65
10	0.148 098 9131(−3)	0.13(−11)	0.17	3	0.148 098 9144(−3)	0.13(−15)	0.67
8	0.366 428 1576(−3)	0.92(−11)	0.14	4	0.366 433 5142(−3)	0.28(−10)	1.18
14	0.794 299 2193(−2)	0.39(−08)	0.29	6	0.794 299 2104(−2)	0.49(−10)	2.54
14	0.697 423 0629(0)	0.51(−08)	0.32	6	0.697 422 9817(0)	0.86(−07)	2.82

$R_2, \zeta_1, \zeta_2, s, v, n_\gamma, n_x, \lambda, R_1$ and v are given in table 3. The values $\tilde{\mathcal{I}}(s)^c$ were obtained using $\bar{D}_n^{(2)}$. The values $\tilde{\mathcal{I}}(s)^d$ were obtained using $\bar{D}_n^{(4)}$.

The B functions are defined as follows [15, 16]:

$$B_{n,l}^m(\zeta, \vec{r}) = \frac{(\zeta r)^l}{2^{n+l}(n+l)!} \hat{k}_{n-\frac{1}{2}}(\zeta r) Y_l^m(\theta_{\vec{r}}, \varphi_{\vec{r}}) \tag{2}$$

where $\hat{k}_{n-\frac{1}{2}}(z)$ stands for the reduced Bessel function [14, 16].

A useful property satisfied by $\hat{k}_{n+\frac{1}{2}}(z)$ is given by

$$\left(\frac{\mathrm{d}}{z\,\mathrm{d}z}\right)^m \left[\frac{\hat{k}_{n+\frac{1}{2}}(z)}{z^{2n+1}}\right] = (-1)^m \frac{\hat{k}_{n+m+\frac{1}{2}}(z)}{z^{2(n+m)+1}}. \tag{3}$$

The Fourier transform $\bar{B}_{n,l}^m(\zeta, \vec{p})$ of $B_{n,l}^m(\zeta, \vec{r})$ is given by [18]

$$\bar{B}_{n,l}^m(\zeta, \vec{p}) = \sqrt{\frac{2}{\pi}} \zeta^{2n+l-1} \frac{(-i|p|)^l}{(\zeta^2 + |p|^2)^{n+l+1}} Y_l^m(\theta_{\vec{p}}, \varphi_{\vec{p}}). \tag{4}$$

The spherical Bessel function $j_l(x)$ of order $l \in \mathbb{N}$ is defined by [42]

$$j_l(x) = (-1)^l x^l \left(\frac{\mathrm{d}}{x\,\mathrm{d}x}\right)^l \left(\frac{\sin(x)}{x}\right). \tag{5}$$

In the following, we write $j_{l+\frac{1}{2}}^n$ with $n = 1, 2, \ldots$, for the successive positive zeros of $j_l(x)$. $j_{l+\frac{1}{2}}^0$ are assumed to be 0.

The three-centre nuclear attraction integrals over STFs are given by

$$\begin{aligned} \mathcal{I}_{n_1,l_1,m_1}^{n_2,l_2,m_2} &= \int_{\vec{R}} \left[\chi_{n_1,l_1}^{m_1}(\zeta_1, \vec{R} - \overrightarrow{OA})\right]^* \frac{1}{|\vec{R} - \overrightarrow{OC}|} \chi_{n_2,l_2}^{m_2}(\zeta_2, \vec{R} - \overrightarrow{OB})\,\mathrm{d}\vec{R} \\ &= \int_{\vec{r}} \left[\chi_{n_1,l_1}^{m_1}(\zeta_1, \vec{r})\right]^* \frac{1}{|\vec{r} - \vec{R}_1|} \chi_{n_2,l_2}^{m_2}(\zeta_2, \vec{r} - \vec{R}_2)\,\mathrm{d}\vec{r} \end{aligned} \tag{6}$$

where A, B and C are three arbitrary points of the Euclidean space $\mathcal{E}_3$, O is the origin of the fixed coordinate system, n_1 and n_2 stand for the principal quantum numbers and where $\vec{r} = \vec{R} - \overrightarrow{OA}$, $\vec{R}_1 = \overrightarrow{AC}$ and $\vec{R}_2 = \overrightarrow{AB}$.

The three-centre nuclear attraction integrals over STFs (6) can be transformed into an analytical expression in terms of the following semi-infinite integrals [19, 20]:

$$\tilde{\mathcal{I}}(s) = \int_0^{+\infty} x^{n_x} \frac{\hat{k}_v[R_2\gamma(s,x)]}{[\gamma(s,x)]^{n_\gamma}} j_\lambda(vx)\,\mathrm{d}x \tag{7}$$

$$= \sum_{n=0}^{+\infty} \int_{j_{\lambda,v}^n}^{j_{\lambda,v}^{n+1}} x^{n_x} \frac{\hat{k}_v[R_2\gamma(s,x)]}{[\gamma(s,x)]^{n_\gamma}} j_\lambda(vx)\,\mathrm{d}x \tag{8}$$

where $j^0_{\lambda,v} = 0$ and $j^n_{\lambda,v} = j^n_{\lambda+\frac{1}{2}}/v$ $(v \neq 0)$ for $n = 1, 2, \ldots$, which are the successive positive zeros of $j_\lambda(vx)$.

In the following, the integrand of $\tilde{\mathcal{I}}(s)$ will be referred to as $\mathcal{F}_s(x)$. In the case when $v \to 0$, the semi-infinite integral (7) vanishes if $\lambda \neq 0$, since $\lim_{\alpha\to 0} j_\lambda(\alpha) = 0$ and the integrand is an exponential decreasing function (converges to 0 when $x \to +\infty$). When $\lambda = 0$, we used the fact that $j_0(\alpha) = \frac{\sin(\alpha)}{\alpha} \to 1$ when $\alpha \to 0$ and that the integrand is an exponentially decreasing function, to obtain the following equation:

$$\tilde{\mathcal{I}}(s) \approx \int_0^{+\infty} x^{n_x} \frac{\hat{k}_v[R_2\gamma(s,x)]}{[\gamma(s,x)]^{n_\gamma}}\,\mathrm{d}x. \tag{9}$$

For the evaluation of the above semi-infinite integral, we used Gauss–Laguerre quadrature of order 64.

With the help of the $S\bar{D}$ approach recently introduced [29], the semi-infinite integral $\tilde{\mathcal{I}}(s)$ (7) can be transformed into a semi-infinite integral involving the simple sine function as follows $(v \neq 0)$ [29]:

$$\tilde{\mathcal{I}}(s) = \frac{1}{v^{\lambda+1}} \int_0^{+\infty} \left[\left(\frac{\mathrm{d}}{x\,\mathrm{d}x}\right)^\lambda \left(x^{n_x+\lambda-1} \frac{\hat{k}_v[R_2\gamma(s,x)]}{[\gamma(s,x)]^{n_\gamma}}\right)\right] \sin(vx)\,\mathrm{d}x \tag{10}$$

$$= \frac{1}{v^{\lambda+1}} \sum_{n=0}^{+\infty} \int_{n\frac{\pi}{v}}^{(n+1)\frac{\pi}{v}} \left[\left(\frac{\mathrm{d}}{x\,\mathrm{d}x}\right)^\lambda \left(x^{n_x+\lambda-1} \frac{\hat{k}_v[R_2\gamma(s,x)]}{[\gamma(s,x)]^{n_\gamma}}\right)\right] \sin(vx)\,\mathrm{d}x. \tag{11}$$

Note that the above infinite series converges faster than the infinite series involving spherical Bessel functions (8) (see tables 1–6).

In the following the integrand of the above semi-infinite integral will be referred to as $\tilde{\mathcal{F}}_s(x)$. It is given by

$$\tilde{\mathcal{F}}_s(x) = G(x)\sin(vx)$$

where the functions $G(x)$ are given by

$$G(x) = \left(\frac{\mathrm{d}}{x\,\mathrm{d}x}\right)^\lambda \left(x^{n_x+\lambda-1} \frac{\hat{k}_v[R_2\gamma(s,x)]}{[\gamma(s,x)]^{n_\gamma}}\right). \tag{12}$$

It is clear that the integrand $\mathcal{F}_s(x)$ in equation (7) oscillates more rapidly than $\tilde{\mathcal{F}}_s(x)$ (see figures 1 and 2). From figures 1 and 2, one can see that the integrand $\tilde{\mathcal{F}}_s(x)$ decays more rapidly than the original integrand $\mathcal{F}_s(x)$, and this may help the extrapolation process.

3. The $S\bar{D}$ approach and the development of the algorithm

The approximation of $\tilde{\mathcal{I}}_s(x)$ obtained using the $S\bar{D}$ approach is given by

$$S\bar{D}_n^{(2,j)} = \frac{1}{v^{\lambda+1}} \frac{\sum_{i=0}^{n+1} \binom{n+1}{i} (1+i+j)^n F(x_{i+j}) \big/ \left[x_{i+j}^2 G(x_{i+j})\right]}{\sum_{i=0}^{n+1} \binom{n+1}{i} (1+i+j)^n \big/ \left[x_{i+j}^2 G(x_{i+j})\right]} \tag{13}$$

where $x_l = (l+1)\frac{\pi}{v}$ for $l = 0, 1, \ldots$ (the successive positive zeros of $\sin(vx)$), $j = 0, 1, 2, \ldots$ and where $F(x) = \int_0^x \tilde{\mathcal{F}}_s(t)\,\mathrm{d}t$.

As can be seen from equation (13), it is necessary to compute the function $G(x)$.

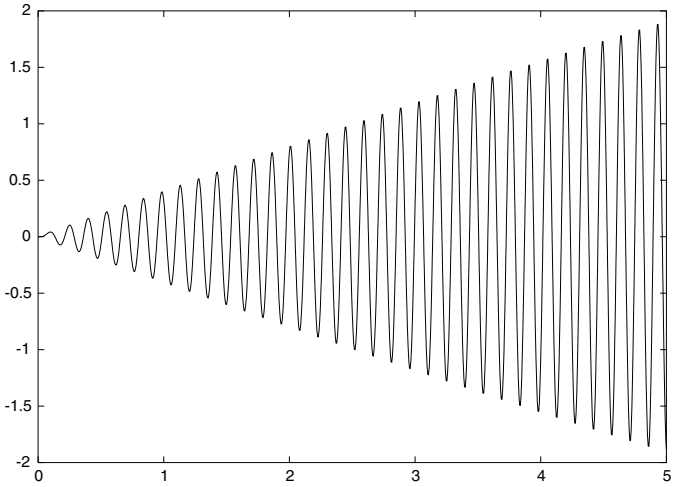

Figure 1. The integrand $\mathcal{F}_s(x)$ of $\tilde{\mathcal{I}}(s)$ (7). $s = 2.40, \nu = 9/2, n_\gamma = 3, n_x = 2, \lambda = 2, R_1 = 45, R_2 = 2, \zeta_1 = 1.5$ and $\zeta_2 = 1$.

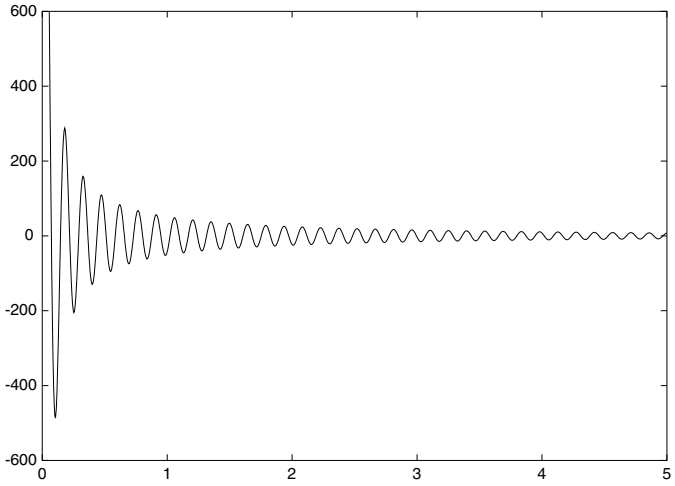

Figure 2. The integrand $\tilde{\mathcal{F}}_s(x)$ of $\tilde{\mathcal{I}}(s)$ (10). $s, \nu, n_\gamma, n_x, \lambda, R_1, R_2, \zeta_1$ and ζ_2 are given in figure (1).

Let $\alpha = n_x + \lambda - 1$. Using Leibnitz formulae and with the help of equation (3) and the fact that $\frac{\mathrm{d}}{\mathrm{d}x} = \frac{\mathrm{d}z}{\mathrm{d}x}\frac{\mathrm{d}}{\mathrm{d}z}$, we obtain for $n_\gamma \neq 2\nu$

$$\left(\frac{\mathrm{d}}{x\,\mathrm{d}x}\right)^{\lambda}\left(x^{\alpha}\frac{\hat{k}_\nu[R_2\gamma(s,x)]}{[\gamma(s,x)]^{n_\gamma}}\right) = \sum_{l=0}^{\lambda}\binom{\lambda}{l}\frac{\alpha!!}{(\alpha-2l)!!}x^{\alpha-2l}\frac{s^{\lambda-l}(1-s)^{\lambda-l}}{[\gamma(s,x)]^{n_\gamma+2(\lambda-l)}}$$
$$\times\sum_{i=0}^{\lambda-l}\binom{\lambda-l}{i}(-1)^{\lambda-l-i}\frac{(2\nu-n_\gamma)!!}{(2\nu-n_\gamma-2i)!!}\hat{k}_{\nu+\lambda-l-i}[R_2\gamma(s,x)] \qquad (14)$$

and for $n_\gamma = 2v$

$$\left(\frac{\mathrm{d}}{x\,\mathrm{d}x}\right)^{\lambda}\left(x^{\alpha}\frac{\hat{k}_v[R_2\gamma(s,x)]}{[\gamma(s,x)]^{2v}}\right)=\sum_{l=0}^{\lambda}(-1)^{\lambda-l}\binom{\lambda}{l}\frac{\alpha!!}{(\alpha-2l)!!}x^{\alpha-2l}$$
$$\times s^{\lambda-l}(1-s)^{\lambda-l}\frac{\hat{k}_{v+\lambda-l}[R_2\gamma(s,x)]}{[\gamma(s,x)]^{2(v+\lambda-l)}}. \tag{15}$$

As can be seen from the above equations, the computation of the function $G(x)$ does not present any difficulty since the value of λ, which depends on l_1 and l_2, cannot be very large.

For the computation of equation (13), we used the following procedure: let $A_k^{(2,j)}$ and $B_k^{(2,j)}$ be defined by

$$\begin{cases} A_k^{(2,j)} = \sum_{i=0}^{k+1}\binom{k+1}{i}(1+i+j)^k F(x_{i+j})\big/\big[x_{i+j}^2 G(x_{i+j})\big] \\ B_k^{(2,j)} = \sum_{i=0}^{k+1}\binom{k+1}{i}(1+i+j)^k \big/\big[x_{i+j}^2 G(x_{i+j})\big]. \end{cases} \tag{16}$$

Equation (13) can now be rewritten as

$$S\bar{D}_k^{(2,j)} = \frac{1}{v^{\lambda+1}}\frac{A_k^{(2,j)}}{B_k^{(2,j)}} \qquad k = 0, 1, 2, \ldots. \tag{17}$$

Let U_i^k be the ith term of the finite sum $A_k^{(2,j)}$. U_i^k is given by

$$U_i^k = \binom{k+1}{i}(1+i+j)^k F(x_{i+j})\big/\big[x_{i+j}^2 G(x_{i+j})\big].$$

Using properties of binomial coefficients, one can easily show that

$$U_i^{k+1} = \frac{(k+2)}{(k+2-i)}(1+i+j)U_i^k. \tag{18}$$

From the above equation, it follows that

$$A_{k+1}^{(2,j)} = \sum_{i=0}^{k+2} U_i^{k+1} = \sum_{i=0}^{k+1}\frac{(k+2)}{(k+2-i)}(1+i+j)U_i^k + U_{k+2}^{k+1}. \tag{19}$$

Now let V_i^k be the ith term of the finite sum $B_k^{(2,j)}$. Using the above arguments, one can easily obtain the following relation for $B_{k+1}^{(2,j)}$:

$$B_{k+1}^{(2,j)} = \sum_{i=0}^{k+2} V_i^{k+1} = \sum_{i=0}^{k+1}\frac{(k+2)}{(k+2-i)}(1+i+j)V_i^k + V_{k+2}^{k+1}. \tag{20}$$

From the above equations, it follows that $S\bar{D}_{k+1}^{(2,j)}$ can be obtained using the following equation:

$$S\bar{D}_{k+1}^{(2,j)} = \frac{1}{v^{\lambda+1}}\frac{\sum_{i=0}^{k+1}\frac{(k+2)}{(k+2-i)}(1+i+j)U_i^k + U_{k+2}^{k+1}}{\sum_{i=0}^{k+1}\frac{(k+2)}{(k+2-i)}(1+i+j)V_i^k + V_{k+2}^{k+1}}. \tag{21}$$

The values of $A_k^{(2,j)}$, $B_k^{(2,j)}$, U_i^k and V_i^k for $k = 0, 1, 2, \ldots$; $i = 0, 1, \ldots, k+1$ are stored at each iteration k of $\left(S\bar{D}_k^{(2,j)}\right)_k$.

Note that the calculation of binomial coefficients is avoided by using the recurrence relations (19) and (20) with equation (21). The most important advantage of using these recurrence relations is the control of the degree of accuracy. In fact, we calculate the

Table 7. Values of $\tilde{\mathcal{I}}(s)$ (7) obtained using $S\bar{D}_n^{(2,0)}$ with recurrence relations. The test (22) was performed to control the degree of the accuracy.

ϵ	s	ν	n_γ	n_x	λ	R_1	v	n	Error
10^{-08}	0.240D−02	9/2	3	2	2	45.00	43.0048	4	0.118D−08
10^{-12}	0.240D−02	9/2	3	2	2	45.00	43.0048	7	0.179D−12
10^{-16}	0.240D−02	9/2	3	2	2	45.00	43.0048	10	0.299D−16
10^{-08}	0.240D−02	5/2	1	1	1	35.00	33.0048	4	0.115D−08
10^{-12}	0.240D−02	5/2	1	1	1	35.00	33.0048	7	0.175D−12
10^{-16}	0.240D−02	5/2	1	1	1	35.00	33.0048	10	0.291D−16
10^{-08}	0.240D−02	9/2	3	2	2	30.00	28.0048	5	0.215D−09
10^{-12}	0.240D−02	9/2	3	2	2	30.00	28.0048	7	0.645D−12
10^{-16}	0.240D−02	9/2	3	2	2	30.00	28.0048	10	0.100D−16

Table 8. Values of $\tilde{\mathcal{I}}(s)$ (7) obtained using $S\bar{D}_n^{(2,0)}$ with recurrence relations. The test (22) was performed to control the degree of the accuracy.

ϵ	s	ν	n_γ	n_x	λ	R_1	v	n	Error
10^{-08}	0.998D+00	9/2	3	2	2	45.00	44.9960	5	0.238D−09
10^{-12}	0.998D+00	9/2	3	2	2	45.00	44.9960	7	0.713D−12
10^{-16}	0.998D+00	9/2	3	2	2	45.00	44.9960	12	0.113D−16
10^{-08}	0.998D+00	5/2	1	1	1	35.00	34.9960	4	0.257D−08
10^{-12}	0.998D+00	5/2	1	1	1	35.00	34.9960	7	0.391D−12
10^{-16}	0.998D+00	5/2	1	1	1	35.00	34.9960	10	0.633D−16
10^{-08}	0.998D+00	9/2	3	2	2	30.00	29.9960	6	0.276D−12
10^{-12}	0.998D+00	9/2	3	2	2	30.00	29.9960	9	0.609D−15
10^{-16}	0.998D+00	9/2	3	2	2	30.00	29.9960	12	0.382D−16

approximation $S\bar{D}_{k+1}^{(2,j)}$ only when the accuracy obtained using $S\bar{D}_k^{(2,j)}$ is not satisfactory. For this we use the following test:

$$\left|S\bar{D}_k^{(2,j)} - S\bar{D}_{k-1}^{(2,j)}\right| = \frac{1}{v^{\lambda+1}}\left|\frac{A_k^{(2,j)}}{B_k^{(2,j)}} - \frac{A_{k-1}^{(2,j)}}{B_{k-1}^{(2,j)}}\right| \leqslant \epsilon \tag{22}$$

where ϵ is defined according to the pre-determined degree of accuracy. If the test is realized, the algorithm stops and returns the approximation $S\bar{D}_k^{(2,j)}$. In tables 7 and 8, we listed values obtained for the semi-infinite integral $\tilde{\mathcal{I}}(s)$ (10) with ϵ varying from 10^{-8} to 10^{-16}, to show the efficiency of the above test.

Note that by using equation (21) and storing the values of U_i^k and V_i^k for $k = 0, 1, 2, \ldots$; $i = 0, 1, \ldots, k+1$, one does not need to calculate all values of $x_{i+j}^2 G(x_{i+j})$ for each order of the $S\bar{D}$. This led to a considerable gain in the calculation times.

A numerical and computation problem occurred in the calculation of the approximations $S\bar{D}_n^{(2,j)}$. In some cases, $G(x_{i+j}) \to 0$.

Let E be the subset of $I = \{0, 1, 2, \ldots, n+1\}$ defined by

$$E = \{k \in I \text{ such that } G(x_{k+j}) \to 0\}.$$

Equation (16) can be rewritten as

$$\begin{cases} A_n^{(2,j)} = \sum_{i\notin E} U_i^n + \sum_{i\in E} U_i^n \\ B_n^{(2,j)} = \sum_{i\notin E} V_i^n + \sum_{i\in E} V_i^n. \end{cases} \tag{23}$$

Now, let us consider $\frac{A_n^{(2,j)}}{B_n^{(2,j)}}$. It is given by

$$\begin{aligned} \frac{A_n^{(2,j)}}{B_n^{(2,j)}} &= \frac{\left[\prod_{l\in E} G(x_{l+j})\right]\sum_{i\notin E} U_i^n + \left[\prod_{l\in E} G(x_{l+j})\right]\sum_{i\in E} U_i^n}{\left[\prod_{l\in E} G(x_{l+j})\right]\sum_{i\notin E} V_i^n + \left[\prod_{l\in E} G(x_{l+j})\right]\sum_{i\in E} V_i^n} \\ &\approx \frac{\sum_{i\in E}\left[\binom{n+1}{i}(1+i+j)^n \frac{F(x_{i+j})}{x_{i+j}^2}\prod_{l\in E, l\neq i} G(x_{l+j})\right]}{\sum_{i\in E}\left[\binom{n+1}{i}(1+i+j)^n \frac{1}{x_{i+j}^2}\prod_{l\in E, l\neq i} G(x_{l+j})\right]}. \end{aligned} \tag{24}$$

$G(x_{i+j}) \to 0$ for all $i \in E$, from this it follows that for all l and k in E:

$$G(x_{l+j}) \approx G(x_{k+j}). \tag{25}$$

Using the above formulae and equation (24), one can easily obtain a very good approximation for $S\bar{D}_n^{(2,j)}$, which is given by

$$S\bar{D}_n^{(2,j)} \approx \frac{1}{v^{\lambda+1}} \frac{\tilde{A}_n^{(2,j)}}{\tilde{B}_n^{(2,j)}} \tag{26}$$

where

$$\begin{cases} \tilde{A}_n^{(2,j)} = \sum_{i\in E} \binom{n+1}{i}(1+i+j)^n \dfrac{F(x_{i+j})}{x_{i+j}^2} \\ \tilde{B}_n^{(2,j)} = \sum_{i\in E} \binom{n+1}{i}(1+i+j)^n \dfrac{1}{x_{i+j}^2}. \end{cases} \tag{27}$$

After a series of numerical tests, we noted that when the above situation happens, the values of $G(x_{i+j})$ are very small for all $i = 0, 1, \ldots, n+1$. Thus, we consider that $E = \{0, 1, 2, \ldots, n+1\}$. Consequently, a good approximation of $S\bar{D}_n^{(2,j)}$ can be obtained by

$$S\bar{D}_n^{(2,j)} \approx \frac{1}{v^{\lambda+1}} \frac{\sum_{i=0}^{n+1}\binom{n+1}{i}(1+i+j)^n F(x_{i+j})/x_{i+j}^2}{\sum_{i=0}^{n+1}\binom{n+1}{i}(1+i+j)^n/x_{i+j}^2}. \tag{28}$$

In our algorithm, the above expression is used when the following conditions are satisfied:

$$R = \left|\frac{A_n^{(2,j)}}{\tilde{A}_n^{(2,j)}} - \frac{B_n^{(2,j)}}{\tilde{B}_n^{(2,j)}}\right| \leqslant \text{tiny} \qquad \text{or} \qquad \tilde{R} = \left|\frac{\tilde{A}_n^{(2,j)}}{A_n^{(2,j)}} - \frac{\tilde{B}_n^{(2,j)}}{B_n^{(2,j)}}\right| \leqslant \text{tiny}. \tag{29}$$

The value of tiny is defined according to the computer used for the calculation. Tiny should be set close to but not identical with the smallest floating point number that is representable on the computer.

Note that the above arguments can also be applied to the case where the values $G(x_{l+j})$ are very large. The test on $\tilde{R}$ treats the case where $G(x_{l+j}) \to +\infty$.

We used equations (21), (26) and (28) for the evaluation of semi-infinite integrals, where the situation $G(x_{i+j})$ is very small for some values of i that occurred (see tables 9 and 10). From the results listed in these tables, one can easily note that the use of (26) and (28) gives very accurate results.

Table 9. Evaluation of $S\bar{D}_{10}^{(2,0)}$ using equations (21), (26) and (28).

i	$G(x_i)$	$S\bar{D}_{10}^{(2,0)}$ (21)	$S\bar{D}_{10}^{(2,0)}$ (26)	$S\bar{D}_{10}^{(2,0)}$ (28)
0	−0.1009(−25)	0.386 333 5913(−3)		0.386 333 5913(−3)
1	−0.2002(−56)	0.386 333 5913(−3)		0.386 333 5913(−3)
2	−0.1636(−86)	0.386 333 5913(−3)		0.386 333 5913(−3)
3	−0.2542(−116)	0.386 333 5913(−3)		0.386 333 5913(−3)
4	−0.5685(−146)	0.386 333 5913(−3)	0.386 333 5913(−3)	0.386 333 5913(−3)
5	−0.1606(−175)	0.386 333 5913(−3)	0.386 333 5913(−3)	0.386 333 5913(−3)
6	−0.5342(−205)	0.386 333 5913(−3)	0.386 333 5913(−3)	0.386 333 5913(−3)
7	−0.2003(−234)	0.386 333 5913(−3)	0.386 333 5913(−3)	0.386 333 5913(−3)
8	−0.8234(−264)	0.386 333 5913(−3)	0.386 333 5913(−3)	0.386 333 5913(−3)
9	−0.3641(−293)	0.386 333 5913(−3)	0.386 333 5913(−3)	0.386 333 5913(−3)
10	−0.1482(−322)	NaN	0.386 333 5913(−3)	0.386 333 5913(−3)
11	0.0000(00)	NaN	0.386 333 5913(−3)	0.386 333 5913(−3)

$s = 0.6650$, $\nu = 17/2$, $n_\gamma = 17$, $n_x = 4$, $\lambda = 3$, $R_1 = 2.50$, $\zeta_1 = 1.50$, $R_2 = 7.00$, $\zeta_2 = 2.00$.

Table 10. Evaluation of $S\bar{D}_{10}^{(2,0)}$ using equations (21), (26) and (28).

i	$G(x_i)$	$S\bar{D}_{10}^{(2,0)}$ (21)	$S\bar{D}_{10}^{(2,0)}$ (26)	$S\bar{D}_{10}^{(2,0)}$ (28)
0	−0.9882(−19)	0.162 057 4878(−3)		0.162 057 4878(−3)
1	−0.1895(−48)	0.162 057 4878(−3)		0.162 057 4878(−3)
2	−0.3368(−79)	0.162 057 4878(−3)		0.162 057 4878(−3)
3	−0.2512(−110)	0.162 057 4878(−3)		0.162 057 4878(−3)
4	−0.1192(−141)	0.162 057 4878(−3)	0.162 057 4878(−3)	0.162 057 4878(−3)
5	−0.4291(−173)	0.162 057 4878(−3)	0.162 057 4878(−3)	0.162 057 4878(−3)
6	−0.1280(−204)	0.162 057 4878(−3)	0.162 057 4878(−3)	0.162 057 4878(−3)
7	−0.3337(−236)	0.162 057 4878(−3)	0.162 057 4878(−3)	0.162 057 4878(−3)
8	−0.7855(−268)	0.162 057 4878(−3)	0.162 057 4878(−3)	0.162 057 4878(−3)
9	−0.1707(−299)	0.162 057 4878(−3)	0.162 057 4878(−3)	0.162 057 4878(−3)
10	0.0000(00)	NaN	0.162 057 4878(−3)	0.162 057 4878(−3)
11	0.0000(00)	NaN	0.162 057 4878(−3)	0.162 057 4878(−3)

$s = 0.465\,0$, $\nu = 5/2$, $n_\gamma = 3$, $n_x = 2$, $\lambda = 2$, $R_1 = 2.50$, $\zeta_1 = 1.00$, $R_2 = 5.00$, $\zeta_2 = 2.00$.

4. Numerical discussion

Tables 1–6 contain values of $\tilde{\mathcal{I}}(s)$ (7). The values $\tilde{\mathcal{I}}(s)^{\text{nmax}}$ are obtained with 15 correct decimals using the infinite series with the sine function (11), which we sum until $N = \text{nmax}$ (tables 1 and 4). The values $\tilde{\mathcal{I}}(s)^a$ are obtained using the infinite series with the spherical Bessel function (8) and the values $\tilde{\mathcal{I}}(s)^b$ are obtained using $S\bar{D}_n^{(2,0)}$ with the recurrence relations (21) (tables 2 and 5). The value of ϵ was set to 10^{-10}. Note that one could increase the degree of accuracy by decreasing the value of ϵ (see tables 7 and 8). The values $\tilde{\mathcal{I}}(s)^c$ and $\tilde{\mathcal{I}}(s)^d$ are obtained using $\bar{D}_n^{(2)}$ and $\bar{D}_n^{(4)}$ respectively (tables 3 and 6). From tables 1 and 4, we note that the semi-infinite series with the sine function converges quickly than the infinite series with the spherical Bessel function, and from tables 2, 3, 5 and 6, we note that the $S\bar{D}$ approach is more accurate and rapid than the $\bar{D}$ transformation applied to the semi-infinite integral with spherical Bessel function. We note that $\bar{D}$ was demonstrated to be more efficient than the approaches using Gauss–Laguerre quadrature, the epsilon algorithm of Wynn or Levin's u transform.

The errors listed in tables 2, 3, 5 and 6 are given by

$$\text{Error}^{\alpha} = |\tilde{\mathcal{I}}(s)^{\text{nmax}} - \tilde{\mathcal{I}}(s)^{\alpha}| \qquad \text{for} \quad \alpha = a, b, c \text{ and } d. \tag{30}$$

For the evaluation of the finite integrals involving equations (8), (11) and (13), we separate two cases: $v \geqslant 1$ and $10^{-15} < v < 1$.

1. When $v \geqslant 1$, we used Gauss–Legendre quadrature of order 20.
2. When $10^{-15} < v < 1$, we divided the finite interval $[x_{i-1}, x_i]$ into M subintervals, where $M = \min(v^{-1}, 100)$. The finite integral can be rewritten as

$$\int_{x_{i-1}}^{x_i} f(t)\,\mathrm{d}t = \sum_{k=1}^{M} \int_{\tilde{x}_{k-1}}^{\tilde{x}_k} f(t)\,\mathrm{d}t \tag{31}$$

where $\tilde{x}_k = x_{i-1} + k\frac{x_i - x_{i-1}}{M}$ for $k = 1, 2, \ldots, M-1$, $\tilde{x}_0 = x_{i-1}$ and $\tilde{x}_M = x_i$. For the evaluation of each finite integral involving in the above finite sum, we used Gauss–Legendre quadrature of order 20.

The value of M was determined after a series of numerical tests on different values of v.

In the case where $10^{-15} < v < 1$, we also used Gauss–Legendre quadrature of order 256 for the evaluation of values of the finite integrals involving equations (8) and (11) without dividing the finite interval to compare the two approaches. The numerical results obtained showed that the first approach is more accurate than increasing the order of Gauss–Legendre to 256.

We note that the calculations are performed for large values of v (tables 1–3) and in the regions where s is very close to 0 and 1 (tables 1–6), where the oscillations are very strong. In tables 4–6, the calculations are performed for small values of v to show that in this case the algorithm described in the present work is still highly efficient. The calculation times listed in tables 1–6 are in milliseconds. Tables 7 and 8 contain values obtained for $\tilde{\mathcal{I}}(s)$ (7) using $S\bar{D}_n^{(2,0)}$ for different values of ϵ which occurs in the test given by (22). Tables 9 and 10 contain values obtained for $S\bar{D}_n^{(2,0)}$ by using equations (21), (26) and (28). From these two tables, we note that when values of $G(x_{i+j})$ are very small, using equations (26) and (28) gives accurate results. From these tables we note that $S\bar{D}_9^{(2,0)}$ and $S\bar{D}_{10}^{(2,0)}$ from equation (21) do not give any values, due to the fact that $G(x_{10})$ and $G(x_{11})$ are considered as 0 by the machine.

For the numerical evaluation of Gaunt coefficients which occur in the complete expression of the three-centre nuclear attraction integrals, we used the subroutine GAUNT.F developed by Weniger and Steinborn [43]. The spherical harmonics $Y_l^m(\theta, \varphi)$ are computed using the recurrence formulae presented in [43].

For the evaluation of the complete expression of the three-centre nuclear attraction integrals over B functions and over STFs (tables 12–14), we used $S\bar{D}$ with the recurrence relations (21) (Values^a). For the evaluation of the finite integrals involved in the expression of $S\bar{D}_n^{(2,0)}$, we used the approach described above. For the evaluation of the outer s finite integrals, we used Gauss–Legendre quadrature of order 48. The value of epsilon ϵ (22) was set to 10^{-15}.

Table 11 contains values obtained for the complete expression of the three-centre nuclear attraction integral over B functions. Values^b were obtained by Grotendorst and Steinborn [20].

In tables 12, 13 and 14, three-centre nuclear attraction integrals over STFs (6) are evaluated. The values are obtained with the NCCH (table 12), NCCCH (table 13) and with linear and nonlinear systems (table 14). Values^b were obtained by Bouferguene *et al* [11, 12, 21]. Values^c were obtained with the Alchemy package [40] (tables 12 and 13).

Table 11. Values obtained for $\mathcal{I}^{n_2,l_2,m_2}_{n_1,l_1,m_1}$ over B functions.

n_1	l_1	m_1	ζ_1	n_2	l_2	m_2	ζ_2	R_1	R_2	Values[a]	Values[b]
1	0	0	1	1	0	0	1	2.0	1.5	0.292 219 986(−1)	0.292 220 008(−1)
1	0	0	1	1	0	0	1	2.0	10.0	0.419 890 811(−4)	0.419 894 695(−4)
5	0	0	1	1	0	0	1	1.5	2.0	0.824 711 574(−2)	0.824 711 555(−2)
5	0	0	1	1	0	0	1	10.0	2.0	0.158 775 768(−2)	0.158 690 139(−2)
1	0	0	1	1	0	0	1	0.5	2.0	0.281 222 107(−1)	0.281 222 151(−1)
1	0	0	1	1	0	0	5	0.5	2.0	0.400 999 465(−3)	0.400 999 369(−3)
3	3	2	1	3	3	2	5	0.5	2.0	0.261 739 704(−8)	0.261 739 704(−8)
1	0	0	1	5	4	4	5	0.5	2.0	0.621 915 968(−5)	0.621 916 063(−5)
1	1	0	1	1	0	0	1	0.5	2.0	0.156 906 773(−2)	0.156 906 740(−2)

$\vec{R}_1 = (R_1, 90^\circ, 0^\circ)$ and $\vec{R}_2 = (R_2, 90^\circ, 0^\circ)$.
[a] Values obtained using $S\bar{D}$ with the recurrence relations.
[b] Values obtained by Grotendorst and Steinborn [20].

Table 12. Three-centre nuclear attraction integrals over STFs (6). Values obtained with the linear molecule NCCH, using the following geometry: $N(0, 0, 0)$, $C_1(2.1864$ au, $0, 0)$, $C_2(4.7980$ au, $0, 0)$ and $H(9.0689$ au, $0, 0)$.

$\mathcal{I}^{\tilde{n}_2,l_2,m_2}_{\tilde{n}_1,l_1,m_1}$	ζ_1	ζ_2	Values[a]	Values[b]	Values[c]
$\langle 1s^N \vert (r_{NC^1})^{-1} \vert 1s^{C_2}\rangle$	8.93	5.23	0.550 116 114(−10)	0.550 082 293(−10)	0.550 082 316(−10)
$\langle 1s^N \vert (r_{NC^1})^{-1} \vert 2p_z^{C_2}\rangle$	8.93	1.25	−0.296 504 029(−02)	−0.296 504 016(−02)	−0.296 503 961(−02)
$\langle 1s^{C_1} \vert (r_{C^{13}})^{-1} \vert 1s^H\rangle$	5.23	0.98	0.169 488 048(−03)	0.169 488 048(−03)	0.169 488 044(−03)
$\langle 2s^{C_1} \vert (r_{C^{12}})^{-1} \vert 2s^{C^3}\rangle$	1.16	1.16	0.118 891 644(00)	0.118 891 647(00)	0.118 891 649(00)
$\langle 2p_z^{C_1} \vert (r_{C^{12}})^{-1} \vert 2p_z^{C^3}\rangle$	1.25	1.25	−0.188 675 485(00)	−0.188 675 450(00)	−0.188 675 497(00)
$\langle 2p_{+1}^N \vert (r_{NC^1})^{-1} \vert 2p_{+1}^{C^3}\rangle$	1.50	2.72	0.855 582 583(−04)	0.855 582 585(−04)	0.855 582 577(−04)
$\langle 1s^N \vert (r_{NC^1})^{-1} \vert 3d_z^H\rangle$	8.93	1.50	0.289 180 618(−04)	0.289 180 603(−04)	0.289 180 543(−04)
$\langle 1s^N \vert (r_{NC^3})^{-1} \vert 3d_z^H\rangle$	8.93	1.50	0.875 086 040(−05)	0.875 085 991(−05)	0.875 085 991(−05)

The abbreviations $2p_{+1}$ and $3d_z$ refer to the Slater functions defined by the quantum numbers: $(n = 2, l = 1, m = 1)$ and $(n = 3, l = 2, m = 0)$. The symbols $(r_{ab})^{-1}$ and $(r_{a^{ij}})^{-1}$ refer to the Coulomb operator $1/|\vec{R} - \overrightarrow{OC}|$ (6).
[a] Values: obtained using $S\bar{D}$ with the recurrence relations.
[b] Values: obtained by Bouferguene and Rinaldi [11].
[c] Values: obtained with the Alchemy package [40].

Table 13. Three-centre nuclear attraction integrals over STFs (6). Values obtained with the linear molecules NCCCH.

$\mathcal{I}^{\tilde{n}_2,l_2,m_2}_{\tilde{n}_1,l_1,m_1}$	ζ_1	ζ_2	Values[a]	Values[b]	Values[c]
$\langle 1s \vert 1s\rangle$	8.93	5.23	0.842 367 256(−5)	0.837 421 476(−5)	0.842 367 013(−5)
$\langle 2p_{+1} \vert 2p_{+1}\rangle$	1.50	1.25	0.561 824 440(−1)	0.561 824 166(−1)	0.561 824 451(−1)
$\langle 2p_{+1} \vert 2p_{+1}\rangle$	3.26	2.72	0.776 215 766(−2)	0.776 204 967(−2)	0.776 215 805(−2)
$\langle 3d_z \vert 3d_z\rangle$	1.95	2.10	−0.160 779 345(−2)	−0.160 660 695(−2)	−0.160 780 598(−2)
$\langle 1s \vert 2p_z\rangle$	8.93	1.25	−0.809 012 412(−2)	−0.800 799 970(−2)	−0.809 012 286(−2)

The abbreviations $2p_{+1}$ and $3d_z$ refer to the Slater functions defined by the quantum numbers: $(n = 2, l = 1, m = 1)$ and $(n = 3, l = 2, m = 0)$. The values are obtained with the geometrical parameters: $\vec{R}_1 = (9.068\,90$ au, $0, 0)$ and $\vec{R}_2 = (2.186\,40$ au, $0, 0)$.
[a] Values: obtained using $S\bar{D}$ with the recurrence relations.
[b] Values: obtained by Bouferguene *et al* [21].
[c] Values: obtained with the Alchemy package [40].

Table 14. Comparison to previous values for linear and nonlinear systems. In this table, the orbitals are assumed to be on the Z axis, i.e., $A(0, 0, 0)$ and $B(0, 0, b)$. Numbers in parentheses represent powers of 10.

Geometry	$\mathcal{I}^{\tilde{n}_2,l_2,m_2}_{\tilde{n}_1,l_1,m_1}$	ζ_1	ζ_2	Values[a]	Values[b]
$b = 5$, $C(-2,5,4)$	$\langle 2s\|2p_z\rangle$	3	3	−0.133 358 289(−3)	−0.133 358 317(−3)
$b = 5$, $C(-3,6,5)$	$\langle 2s\|2p_z\rangle$	3	3	−0.104 521 855(−3)	−0.104 521 843(−3)
$b = 5$, $C(-4,7,6)$	$\langle 2s\|2p_z\rangle$	3	3	−0.853 195 531(−4)	−0.853 195 527(−4)
$b = 2$, $C(0,0,9)$	$\langle 2s\|1s\rangle$	4	1	0.263 024 091(−1)	0.263 024 091(−1)
$b = 5$, $C(0,0,9)$	$\langle 2s\|1s\rangle$	4	1	0.153 828 015(−2)	0.153 828 015(−2)
$b = 8$, $C(0,0,9)$	$\langle 2s\|1s\rangle$	4	1	0.794 563 791(−4)	0.794 563 815(−4)

[a] Values: obtained using $S\bar{D}$ with the recurrence relations.
[b] Values: obtained by Bouferguene and Jones [12].

The accuracy in the numerical evaluation of the complete expression of the three-centre nuclear attraction integral depends strongly on the accuracy in the evaluation of the semi-infinite integrals. From tables 1–6, one can note that the algorithm described in the present work lead to highly accurate results and to a substantial reduction in the calculation times.

The values listed in tables 11–14 are in agreement with those obtained by Grotendorst and Steinborn [20] (nine similar decimals in most cases), by Bouferguene *et al* [11, 12, 21] (ten similar decimals in most cases in table 12, 6 in table 13 and more than ten in table 14). A comparison with the values obtained with the Alchemy package [40] showed that in most cases we obtained ten similar decimals (tables 12 and 13).

All the calculations were performed on a PC Workstation Intel Xeon Processor 2.4 GHz using Lahey/Fujitsu Fortran compiler (LF95 PRO v5.7).

5. Conclusion

Three-centre nuclear attraction integrals over STFs are most frequently encountered in any *ab initio* molecular orbital (MO) calculations based on LCAO-MO. The computation of these integrals is one of the most difficult and time consuming steps in molecular systems calculation.

Analytic expressions can be obtained for these integrals by choosing the B functions as a basis set of atomic orbitals and applying the Fourier transform method. These analytic expressions turned out to be extremely difficult to evaluate because of the presence of highly oscillatory semi-infinite integrals whose integrands involve spherical Bessel functions.

We showed that these semi-infinite integrals involving spherical Bessel functions can be transformed into semi-infinite integrals involving the simple sine function and satisfy all the conditions to apply $\bar{D}$. The use of Cramer's rule for calculating approximations of semi-infinite integrals under consideration was possible with the help of properties of the sine function.

An efficient algorithm based on $S\bar{D}$ is now developed for a fast numerical evaluation of the semi-infinite integrals which occur in the analytic expression of the three-centre nuclear attraction integrals over B functions. The complete expressions of the integral over B functions and over STFs are evaluated using the new algorithm. The numerical results that we obtained showed the gain in the calculation times realized for a high accuracy.

References

[1] Clementi E 1989 *Modern Techniques in Computational Chemistry* (Leiden: ESCOM)
[2] Roothaan C C 1951 *Rev. Mod. Phys.* **23** 69

[3] Agmon S 1985 Bounds on exponential decay of eigenfunctions of Schrödinger operators *Schrödinger Operators* ed S Graffi (Berlin: Springer)
[4] Kato T 1957 *Commun. Pure Appl. Math.* **10** 151
[5] Boys S F 1960 *Proc. R. Soc.* A **258** 402
[6] Slater J C 1930 *Phys. Rev.* **36** 57
[7] Slater J C 1932 *Phys. Rev.* **42** 33
[8] Kutzelnigg W 1988 *J. Mol. Struct. (THEOCHEM)* **50** 33
[9] Bouferguene A, Fares M and Hoggan P E 1996 *Int. J. Quantum Chem.* **57** 801
[10] Weatherford C A and Jones H W 1981 *ETO Multicenter Molecular Integrals* (Dordrecht: Reidel)
[11] Bouferguene A and Rinaldi D 1994 *Int. J. Quantum Chem.* **50** 21
[12] Bouferguene A and Jones H W 1998 *J. Chem. Phys.* **109** 5718
[13] Rico F J, Lòpez R, Aguado A, Ema I and Ramìrez G 1998 *Int. J. Quantum Chem.* **19** 1284
[14] Shavitt I 1963 The Gaussian function in calculation of statistical mechanics and quantum mechanics *Methods in Computational Physics vol 2. Quantum Mechanics* ed B Alder, S Fernbach and M Rotenberg (New York: Academic)
[15] Filter E and Steinborn E O 1978 *Phys. Rev.* A **18** 1
[16] Steinborn E O and Filter E 1975 *Theor. Chem. Acta* **38** 273
[17] Weniger E J and Steinborn E O 1989 *J. Math. Phys.* **30** 774
[18] Weniger E J and Steinborn E O 1983 *J. Chem. Phys.* **78** 6121
[19] Trivedi H P and Steinborn E O 1983 *Phys. Rev.* A **27** 670
[20] Grotendorst J and Steinborn E O 1988 *Phys. Rev.* A **38** 3857
[21] Bouferguene A, Fares M and Rinaldi D 1994 *J. Chem. Phys.* **100** 8156
[22] Steinborn E O, Homeier H H H, Ema I, Lòpez R and Ramìrez G 2000 *Int. J. Quantum Chem.* **76** 244
[23] Safouhi H, Pinchon D and Hoggan P E 1998 *Int. J. Quantum Chem.* **70** 181
[24] Safouhi H and Hoggan P E 1998 *J. Phys. A: Math. Gen.* **31** 8941
[25] Safouhi H and Hoggan P E 1999 *J. Phys. A: Math. Gen.* **32** 6203
[26] Safouhi H and Hoggan P E 1999 *J. Math. Chem.* **25** 259
[27] Safouhi H and Hoggan P E 1999 *J. Comput. Phys.* **155** 331
[28] Safouhi H 2000 *J. Comput. Phys.* **165** 473
[29] Safouhi H 2001 *J. Phys. A: Math. Gen.* **34** 2801
[30] Safouhi H 2002 *J. Comput. Phys.* **176** 1–19
[31] Safouhi H 2001 *J. Phys. A: Math. Gen.* **34** 881
[32] Sidi A 1980 *J. Inst. Maths. Appl.* **26** 1
[33] Sidi A 1997 *J. Comput. Appl. Math.* **78** 125
[34] Sidi A 1979 *J. Inst. Math. Appl.* **24** 327
[35] Levin D and Sidi A 1981 *Appl. Math. Comput.* **9** 175
[36] Sidi A 1982 *Numer. Math.* **38** 299
[37] Sidi A 1982 *Math. Comp.* **38** 517
[38] Ford W F and Sidi A 1987 *SIAM J. Numer. Anal.* **24** 1212
[39] Sidi A 1988 *Math. Comput.* **51** 249
[40] Yoshimine M, Lengsfield B H, Bagus P S, McLean B and Liu B 1990 *Alchemy II (International Business Machines San Jose, from MOTECC-90)*
[41] Condon E U and Shortley G H 1970 *The Theory of Atomic Spectra* (Cambridge: Cambridge University Press)
[42] Arfken G B and Weber H J 1995 *Mathematical Methods for Physicists* 4th edn (New York: Academic)
[43] Weniger E J and Steinborn E O 1982 *Comput. Phys. Commun.* **25** 149